Control of tongue movements by the Purkinje cells of the cerebellum

Paul Hage, Mohammad Amin Fakharian, Alden M. Shoup, Jay S. Pi, Ehsan Sedaghat-Nejad, Simon P. Orozco, In Kyu Jang, Vivian Looi, Toren Arginteanu, and Reza Shadmehr

Laboratory for Computational Motor Control, Dept. of Biomedical Engineering, Johns Hopkins School of Medicine, Baltimore, Maryland 21205, USA

Correspondence: Reza Shadmehr, Johns Hopkins School of Medicine, 410 Traylor Building, 720 Rutland Ave., Baltimore, MD 21205. Email: shadmehr@jhu.edu

Acknowledgements: The work was supported by grants from the National Science Foundation (CNS-1714623), and the NIH (R01-EB028156, R37-NS128416).

Author contributions: PH and RS conceived experiments. PH, MAF, AMS, JSP, ESN, and SPO collected the data. PH, MAF, IKJ, VL, and RS analyzed the data. PH made the figures and performed statistical analysis. RS wrote the manuscript.

Competing interests: None.

Data availability: https://osf.io/WDXU4/

ORCID ID: Paul Hage 0000-0002-7006-9877, Mohammad Amin Fakharian 0000-0002-7741-8689, Alden Shoup 0000-0003-1206-6587, Simon Orozco 0000-0001-6092-7228, Jay Pi 0000-0003-4036-2877, Ehsan Sedaghat-Nejad 0000-0001-6732-1296, In Kyu Jang 0000-0002-1832-3743, Vivian Looi 0000-0002-9392-4178, Toren Arginteanu, 0000-0002-6029-7323, Reza Shadmehr 0000-0002-7686-2569.

Abstract

To quantify the cerebellum's contributions to control of the tongue, we trained head-fixed marmosets to make dexterous movements, harvesting food from small tubes that were placed orthogonal to the mouth. We identified the lingual regions in lobule VI of the vermis and recorded from hundreds of Purkinje cells (P-cells), each in sessions where the subject produced thousands of licks. Most movements aimed for one of the small tubes, while other movements groomed the mouth area. To quantify contributions of a P-cell to control of the tongue, we relied on the fact that in a small fraction of the licks, the input from the inferior olive produced a complex spike (CS), which then briefly but completely silenced the P-cell. When the movements were targeting a tube, the CS rates increased during protraction for both ipsilateral and contralateral targets, thus identifying the preferred axis of motion in the olivary input, termed CS-on. However, for grooming movements this modulation was absent. We compared the tongue's trajectory in the targeted movement that had experienced the CS with temporally adjacent targeted licks that had not. When the SS suppression occurred during protraction, the tongue exhibited hypermetria, and when the suppression took place during retraction, the tongue exhibited slowing. These effects amplified when two P-cells were simultaneously suppressed. Therefore, CS-induced suppression of P-cells in the lingual vermis disrupted the forces that would normally decelerate the tongue as it approached the target, demonstrating a specialization in stopping the movement. Because the CS-on direction tended to align with the direction of downstream forces produced during P-cell suppression, this suggests that for targeted licks, the olivary input defined an axis of control for the P-cells.

Significance statement

During dexterous licking, a CS-induced suppression of P-cells in the lingual vermis inhibited the forces that would otherwise retract the tongue, resulting in hypermetria during protraction and slowing during retraction. Because the direction of these forces aligned with the direction of motion specified by the olivary input, a pattern that is also present for P-cells in the oculomotor region of the cerebellum, the results imply a general computation for P-cells during control of targeted movements.

Introduction

We use our tongue for verbal communication and mastication, skills that require the brain to control more than 100 muscles simultaneously (1). Damage to the cerebellum disrupts these movements, resulting in abnormal muscle activation patterns (2) that bear a resemblance to ataxia of the arm (3). Indeed, life without a cerebellum in humans (4), or inactivation of the deep cerebellar nuclei in mice (5), do not eliminate tongue movements. Rather, the movements become inaccurate. For example, if the activities of Purkinje cells (P-cell) are disrupted via silencing of molecular layer interneurons, the tongue's trajectory becomes erratic and the subject is no longer able to efficiently harvest liquid rewards (6). Thus, the role of the cerebellum in control of the tongue may be similar to its function during control of the limbs and the eyes: stopping the movement on target. But how might the cerebellum achieve this?

In primates, stimulation of the fastigial nucleus moves the tongue predominantly in the ventral-dorsal axis, while stimulation of the dentate nucleus moves it mainly in the lateral-medial axis (7). Notably, tongue muscles are most readily activated through stimulation of the fastigial nucleus (as compared to the other cerebellar nuclei) (8), suggesting that the P-cells that are located in the vermis play a prominent role in control of the tongue. Unfortunately, there are no published reports of P-cell activity in the vermis during targeted tongue movements in any species, but more is known regarding activity of P-cells in Crus I and Crus II regions (in rodents). For example, before start of a bout, many P-cells in Crus I and Crus II show an increase in their simple spikes (SS), while a smaller number show a decrease (9). Once the licking begins, the SS rates as a population are phase-locked to the rhythm of the lick, with rate maxima occurring near lick onset (5). Complex spikes (CSs) also exhibit their highest rates during protraction (9, 10). The challenge is to understand the relationship between the activities of P-cells and control of the tongue.

Here, we explored this question in marmosets, as they not only have a long tongue (21 mm long, 8 mm wide) (11), but they are also skillful in using it, burrowing into small tree holes, extracting sap and insects. We trained head-fixed marmosets to make thousands of tongue movements to harvest food from small tubes that were placed at 90° to the mouth. We then relied on the fact that the inferior olive not only transmits unexpected sensory events to the cerebellum (12–15), it also transmits information regarding the direction of the planned movement (15, 16). The result is a complex spike that briefly but completely suppresses the P-cell (17, 18), resulting in a movement (19), or disruption of the ongoing movement (20, 21). Thus, the CS events provide an opportunity to ask whether the resulting P-cell suppression is followed by a change in control of the tongue. Indeed, SS suppression disrupted the deceleration phase as the tongue approached the target, as well as the retraction phase as it returned to the mouth.

Regardless of whether the target of the movement was ipsilateral or contralateral to the location of the recording, as a population the CS rates were highest during protraction, termed CS-on. Critically, the CS-on direction of the P-cells, extension of the tongue, coincided with the direction of downstream forces that their SS suppression induced on the tongue's trajectory, protraction. Thus, the encoding of the sensorimotor space by the climbing fiber input coincided with the downstream effects that the SS suppression had on control of the tongue. Because a similar phenomenon is present among P-cells that contribute to control of the eyes (15, 21), our results suggest that across disparate types of movements, the inferior olive imposes a consistent architecture of control upon the cerebellum.

Results

We tracked the eyes and the tongue of head-fixed marmosets (n=3) as they performed visually guided saccades in exchange for food (Fig. 1A). The subjects performed a sequence of saccades, at the end of which we delivered an increment of food (slurry mixture of apple sauce and monkey chow). This food was presented via either the left or the right tube for 50-300 consecutive trials, and then switched tubes. Because the amounts were small (0.015-0.02 mL), and the tubes were located at ±90° with respect to the mouth, harvesting was effortful (22), requiring skillful movements toward a target that was just large enough to accommodate the tongue (4.4 mm diameter tube). As a result, the subjects naturally chose to work for a few consecutive saccade trials (n=6.1±0.02 successful trials per work period), allowing the food to accumulate, then stopped making saccades to targets and initiated their harvest via a bout of licking (n=22.03 ± 0.04 licks per harvest period, Fig. 1B).

The tongue movements were of two general types: in the task relevant licks the subjects aimed for the tube, whereas in the task irrelevant licks the subjects groomed their mouth (Fig. 1A). We further divided the task relevant licks into two subtypes, those that touched the edge of the tube and harvested the food that was near the tip (Fig. 1A, labeled 2&4), and those that penetrated the tube and harvested the food that was deeper (Fig. 1A, labeled 1&5). During a typical 2-3 hour recording session, the subjects performed n=4401±11 task relevant licks (i.e., aimed at a tube, mean±SEM), and n=1310±4 task irrelevant licks (Supplementary Fig. 1). We tracked the motion of the tongue in the horizontal plane using DeepLabCut (23), and combined MRI and CT image guided procedures (24) to place heptodes and silicon probes in lobule VI of the vermis. Over the course of 3.5 years, we recorded from n=284 P-cells (Fig. 1C, Supplementary Fig. 2). A neuron was identified as a definitive P-cell (n=230) because of the presence of complex spikes (CS). In addition, we included data from putative P-cells (n=54) for which we could not isolate the CSs but the neuron was located in the P-cell layer and exhibited 0 ms synchronous simple spike (SS) interactions with other confirmed P-cells (15, 16, 25).

Fig. 1D illustrates the activities of two P-cells. One P-cell increased its SS activity before bout onset, earlier when the tongue targeted the ipsilateral tube, while another P-cell decreased its SS activity, earlier for the contralateral tube (with respect to the site of recording). As the bout began, the CS rates appeared to increase briefly in both P-cells while the SS rates were modulated in a rhythmic pattern that appeared related to tongue kinematics. We focused on three periods during each lick: protraction acceleration period (Fig. 1D, a-b), protraction deceleration period (b-c), and retraction acceleration period (c-d). We then quantified the relationship between the spikes that were generated by a given P-cell and its downstream effects on the motion of the tongue.

The CS-induced SS suppression resulted in overshooting of the tongue during protraction, and slowed return during retraction

As a population, the n=230 confirmed P-cells exhibited CS rates that increased near the onset of protraction (Figs. 2A), peaking around the time the tongue touched the tube, and then decreased below baseline near retraction onset. The rate increases during protraction were larger for ipsilateral licks (within cell difference, protraction period, mean±SEM: 0.077±0.024, t(229)=26.7, p=1.9E-72). Thus, as a population, for both target directions, the CS-on was protraction of the tongue, whereas the CS-off direction was retraction.

As expected, the olivary input suppressed the P-cell's SS production (Fig. 2B, left: all P-cells, right: single P-cell), lasting an average of 14.8±0.44 ms during licking (time to 85% recovery of SS rate, mean±SEM). However, the CS events were rare: a CS occurred in only 5.45±0.01% of the licks during protraction acceleration period (mean±SEM), 9.28±0.01% of the licks during protraction deceleration period, and 6.59±0.009% of the licks during retraction acceleration period (Fig. 2C). We collected a large number of licks per neuron (4401±11 licks, Fig. 2D) and then asked whether the CS-induced SS suppression affected the motion of the tongue.

For each P-cell we considered triplets of consecutive licks $\{n-1, n, n+1\}$ in which all three licks were of the same type, i.e., contacted the same part of the tube (edge or inner). We then selected the subset of triplets in which there was a CS at only a single period in lick n, but no CS during any period in the two neighboring licks $n-1$, and $n+1$. For example, consider tongue trajectories in which there was a CS in one P-cell during the acceleration period of protrusion (Fig. 3A). This acceleration period was brief (49.9±0.019 ms), during which the SS activity was normally rising and nearly identical in licks $n-1$ and $n+1$ (Fig. 3B, 1st row), but suppressed during lick n. We measured the change in SS activity by comparing lick n with licks $n-1$ and $n+1$ and plotted the results of each comparison in Fig. 3B, green & blue solid lines (labeled suppressed, top row, right column). As a control, we performed a bootstrapping procedure in which we generated a pseudo data set for each P-cell by randomly assigning the CS label to a lick and comparing it with its two temporally adjacent neighbors. As expected, in trials in which there was a CS, the SSs were suppressed during the acceleration period of protraction, but then rapidly recovered.

To ask whether there were any effects of this brief SS suppression on tongue kinematics, we measured the distance of the tongue tip to the mouth, and also its angle with respect to the midline, and then compared the SS suppressed trajectories with the neighboring licks in which a CS was absent. The effects appeared consistent among the P-cells (Fig. 3A, red colors): following SS suppression, the tongue was slightly displaced toward the target. Statistical testing, however, which relied on bootstrapping procedure to compute 95% confidence intervals (CI), demonstrated that the changes were within the error bounds. That is, the CS-induced suppression during the acceleration period of protraction had no significant effects on tongue trajectory (Fig. 3C, measured via distance to the mouth, and its angle, at peak protraction speed and peak displacement).

However, as the protraction proceeded, the effects of SS suppression increased. If the suppression occurred during the deceleration period of protraction (103.6±0.04 ms), the tongue exhibited hypermetria (Fig. 3E, second row), producing increased displacement and increased angle of the tongue's trajectory (Figs. 3F, displacement: 0.37±0.002 mm, 95%CI = [-0.45 0.26] mm, angle: 3.35±0.02 deg, 95%CI = [-2.89 2.30] deg). Notably, the effects were similar regardless of whether lick n was compared to the previous lick ($n-1$), or the subsequent lick ($n+1$) (Fig. 3E, second row, blue and green traces). Moreover, the effects were consistent across the P-cells (Fig. 3D, red colors, also Supplementary Figure 3, left panel), but larger for contralateral licks (within cell difference, ipsilateral minus contralateral, at lick endpoint, displacement mean±SEM: -0.15±0.04 mm, t(229)=-3.97, p=9.6E-05, angle: -1.41±0.37, t(229)=-3.79, p=9.69E-05).

These results hinted that SS suppression prevented normal deceleration, producing hypermetria in the direction of the target. If this interpretation is valid, then a similar suppression during the retraction period should produce forces that are again in the direction of protraction, now impeding the

tongue's return. That is, if SS suppression during protraction sped the outward movement, then the same suppression during retraction should slow the inward movement.

As retraction began, the population CS activity (Fig. 2A) had fallen below baseline, i.e., opposite of the activity during protraction. Yet, if the CS occurred during the acceleration period of retraction (78.3±0.02 ms), the resulting suppression was again an outward displacement of the tongue (Fig. 3G). Indeed, comparison of lick n with $n-1$ or $n+1$ revealed a consistent effect: an increased distance and angle of the tongue to the mouth (Fig. 3I, displacement: 1.29±0.002 mm, 95%CI = [-0.71 0.69] mm, angle: 4.70±0.02 deg, 95%CI = [-3.18 3.21] deg). These effects were present for ipsilateral and contralateral licks (Fig. 3H), larger for the contralateral licks (within cell difference, ipsilateral minus contralateral, at lick endpoint, displacement: -0.37±0.09 mm, t(229)=-3.97, p=4.8E-05, angle: -2.06±0.50, t(229)=-4.1, p=2.71E-05), and consistent across the P-cells (Fig. 3G, red colors). The effect of suppression on lick trajectory for each P-cell is shown in Supplementary Figure 3, right panel. Thus, the CS-induced SS suppression during retraction slowed the return of the tongue.

In summary, when a CS-induced SS suppression occurred during the deceleration period of the tongue's protrusion, the tongue overextended toward the target. When this suppression occurred during retraction, the tongue's return was slowed. These effects were present for targets on both the ipsilateral and contralateral sides, but greater when the target was contralateral to the recording. Thus, it appeared that SS suppression disrupted the motor commands that would normally stop the tongue during protraction and return the tongue during retraction.

Perturbations scaled when pairs of P-cells were simultaneously suppressed

Our dataset included n=298 pairs of simultaneously recorded P-cells. This provided the opportunity to test whether near simultaneous suppression of 2 P-cells had a greater effect on tongue kinematics as compared to when only one of the two P-cells was suppressed.

As before, we collected triplets of consecutive licks $\{n-1, n, n+1\}$ where all the licks were of the same type (directed toward the same part of the tube), but only lick n had a CS. We divided the triplets based on whether a CS was present in only one of the P-cells, or both P-cells, then computed trajectory differences between licks n and $n-1$, as well as licks n and $n+1$. Finally, for each pair of P-cells we averaged $n-(n-1)$ and $n-(n+1)$ to increase statistical power (because there were far fewer licks in which both P-cells experienced a CS during the same period of the movement).

We found that if the CS occurred in both P-cells during the deceleration phase of protraction, there was significantly greater displacement of the tongue, and its angle, as compared to when only one of the P-cells was suppressed (Fig. 4A, angle: t(248) = -3.7167, p = 2.5E-04, displacement: t(248) = -5.5471,p = 7.43E-08). Similarly, when the suppression occurred during retraction, the return phase of the movement experienced a greater slowing in the case of 2 P-cells as compared to a single P-cell (Fig. 4B, angle: t(192) = 6.34, p = 1.6tE-09, displacement: t(192) = 6.50, p = 6.79E-10). Thus, near simultaneous suppression of 2 P-cells roughly doubled the kinematic effects, further disrupting deceleration and return of the tongue.

Control studies

The fact that a CS was present during a given period in lick n may have been because earlier in the tongue's trajectory there was an event (for example, an error), that affected that movement, increasing

the likelihood of a CS, and resulting in compensatory movements that followed the CS. To check for this, for each period during which we observed a CS we considered the tongue's trajectory in the same lick but during the period preceding the CS. For example, for the licks in which there was a CS in the protraction deceleration period we focused on the acceleration period of the same movement. By comparing the lick in which the CS had occurred with its two neighbors, we found that in the period before the CS had occurred tongue kinematics remained within the 95% confidence intervals of chance: distance to mouth and angle of the tongue at peak speed were not different than chance (Fig. 3F, displacement: -0.11±0.001 mm, 95%CI = [-0.22 0.23] mm, angle: 0.19±0.01 deg, 95%CI = [-1.36 1.45] deg).

Next, we checked the tongue movements in which there was a CS in the retraction period. We compared the tongue's trajectory in the protraction period of the same lick at peak protraction speed, and at peak protraction displacement. We found that before the CS had occurred, at the onset of the retraction the distance to mouth and tongue angle were not different than chance (Fig. 3I, displacement: 0.01±0.002 mm, 95%CI = [-0.37 0.35] mm, angle: 0.68±0.02 deg, 95%CI = [-3.05 2.80] deg). Moreover, during the preceding protraction in the same lick, at peak tongue speed distance and angle were again not different than chance (displacement: -0.66±0.003 mm, 95%CI = [-0.70 0.74] mm, angle:-2.16±0.02 deg, 95%CI = [-3.35 3.58] deg). Yet, if during the return phase a CS was present, the movement was slowed (Fig. 3I, displacement: 1.29±0.002 mm, 95%CI = [-0.71 0.69] mm, angle: 4.70±0.02 deg, 95%CI = [-3.18 3.21] deg). That is, the tongue's trajectory before the CS was not significantly different than the neighboring licks, but after the CS-induced SS suppression the trajectories diverged.

As a further control, we considered movements in which there was a CS event just before protrusion onset (Supplementary Figure 4). In these movements, the SS rates were suppressed, but importantly, the rates recovered around 10 ms after lick onset (Supplementary Figure 4, 1st row). Critically, despite the presence of a CS just before the lick had started, the SS rates during the entire protrusion and retraction periods were indistinguishable from licks that had not. The trajectory of the tongue as measured via distance and angle remained within the 95% confidence interval bounds of chance (Supplementary Figure 4, 3rd and 4th rows).

Effect of SS suppression remained consistent across P-cells regardless of SS modulation

We had observed that for nearly every P-cell, during both protraction and retraction, the CS-induced SS suppression was followed by an extension of the tongue (Figs. 3D & 3G). This consistency was surprising in light of the diversity that was present in the SS patterns: before the onset of the bout, some P-cells had increased their SS rates with respect to baseline, while others had decreased (Fig. 1D). Did the kinematic effects of SS suppression differ in these two groups?

In our data set of n=142 of P-cells with SSs, most cells (n=123) increased their SS rates before the onset of the bout, but a minority exhibited a decrease (n=31) (Figs. 5A and 5B). We separated the P-cells into SS increasers and decreasers and found that despite the differences in their SS patterns, the CS rates increased in both groups near bout onset (Fig. 5C, peak CS firing rate change from baseline, SS increasers: 0.15±0.04 Hz, SS decreasers: 0.26±0.10 Hz). We then compared tongue trajectories in triplets of consecutive licks $\{n-1, n, n+1\}$, finding that during protraction, following SS suppression in the deceleration period, in both groups of P-cells the tongue trajectory was displaced away from the

262 mouth, exhibiting a greater distance and angle (Fig. 5D, displacement: 0.38±0.005 mm, 95%CI = [-0.1
263 0.049] mm, angle: 3.72±0.05 deg, 95%CI = [-0.62 0.43] deg, SS decreasers: displacement: 0.45±0.04 mm,
264 95%CI = [0.04 -0.06] mm, angle: 4.28±0.54 deg, 95%CI = [0.42 -0.45] deg). Similarly, during retraction, SS
265 suppression in both groups of P-cells produced a slowing of the tongue's return, resulting in a greater
266 distance and angle (Fig. 5E, displacement: 1.25±0.01 mm, 95%CI = [-0.12 0.12] mm, angle: 4.45±0.05
267 deg, 95%CI = [-0.53 0.56] deg, SS decreasers: displacement: 1.04±0.04 mm, 95%CI = [0.07 -0.07] mm,
268 angle: 3.48±0.17 deg, 95%CI = [0.37 -0.35] deg).
269 Thus, despite the differences in the patterns of SS activity during licking among the P-cells, the
270 downstream effect of CS-induced SS suppression was consistently an extension of the tongue.
271
272 *The population SS rates encoded parameters of tongue kinematics*
273 In order to organize the P-cells into a population, we relied on the fact that the downstream effects of
274 SS suppression, for both increasers and decreasers, in both ipsilateral and contralateral directions, were
275 to produce forces that extended the tongue. Thus, we combined all cells and computed a population
276 response during various phases of tongue movements.
277 Across the cells, the CS rates peaked at approximately the timepoint of maximum protraction
278 velocity (Figs. 6A, left column), exhibiting a greater rate for movements toward the ipsilateral side
279 (ipsilateral: 0.21±0.02 Hz, contralateral: 0.16±0.02 Hz, within cell difference, average CS rate, ipsilateral
280 minus contralateral, t(229)=28.1, p=2.5E-76). In contrast, the CS rates declined below baseline before
281 the onset of retraction (Fig. 6B, left column). Thus, the CS-on direction across the P-cells was
282 protraction, whereas CS-off was retraction, suggesting that the CS-on direction aligned with the
283 downstream effects of SS suppression.
284 To analyze the SS activities as a population, we had to consider the fact that during a bout, as
285 the SS rates modulated about a mean, the mean was not stationary (Fig. 5A). Rather, the mean SS rates
286 rose or fell before bout onset, then drifted back toward the values before start of the bout, reaching
287 pre-bout levels at bout ended. Thus, to quantify modulation of SS rates, for each P-cell we considered a
288 2 sec moving window to compute the running average of its firing rate, then computed the SS rates with
289 respect to this mean. The 2 sec window was chosen because it was roughly an order of magnitude larger
290 than the duration of a typical lick.
291 If a suppression in SS rates produced downstream forces that pulled the tongue outwards
292 toward the target, then during deceleration the SS rates should increase, thus commanding forces that
293 would stop the motion of the tongue. Indeed, the SS rates peaked near protraction peak speed, and
294 were larger for contralateral licks (Fig. 6A, right column, ipsilateral: 11.58±1.75 Hz, contralateral:
295 12.91±1.95 Hz, within cell difference, t(156)=13.6, p=2.9E-28). The rates began declining at retraction
296 onset and reached a minimum near retraction peak speed (Fig. 6B). To test if this modulation varied
297 with tongue kinematics, we quantified lick vigor, defined as the peak speed of a given protraction with
298 respect to the speed expected for a lick of the same amplitude (22, 26) (Supplementary Figure 5). High
299 vigor licks exhibited greater SS rates at peak protraction speed (Fig. 6D, within cell difference, high vigor
300 minus low vigor, 2.92±0.60 Hz, t(156)=14.1, p=1.2E-29).
301 Given that SS suppression during protraction led to increased extension, if we interpret the
302 increase in SS rates as commanding downstream forces to induce retraction, then the increased SS rates
303 during high vigor licks is consistent with the idea that the P-cells are firing to stop the protrusion. If true,

304 then protractions that have the same peak speed, but a longer deceleration, should not only exhibit
305 greater SS rates at peak speed, but also a longer duration of activity above baseline. Indeed, we found
306 that licks that had similar peek speed but longer decelerations tended to also have a longer period of SS
307 rate increase (Fig. 6F, time to baseline crossing, high duration: 126.80±7.68 ms, low duration:
308 86.02±7.23 ms, paired t-test, t(156)=7.84, p=6.75E-13).
309 All of these results were for tongue movements in which the target was a small tube. Would the
310 same pattern be present for movements that did not require such precision? To answer this question,
311 we turned to the task irrelevant, grooming licks. These licks tended to be slower, with a peak speed that
312 was roughly half the speed of the task relevant movements (Fig. 6E, light and dark shaded regions, task
313 relevant: 290.5±3.6 mm/s, task irrelevant: 153.8±2.5 mm/s). Remarkably, during protraction of the
314 grooming licks the CS rates were essentially at baseline: the CS rates were an order of magnitude
315 smaller than when the movements were task relevant (Fig. 6F, left, paired t-test, reward vs grooming,
316 combined directions, t(229)=-3.27, p=0.00126).
317 Similarly, the SS rates during protraction were much smaller during the task irrelevant
318 movements as compared to the movements that were task relevant (Fig. 6E, right, paired t-test, reward
319 vs grooming, combined directions, t(156)=8.6, p=8.44E-15). In sharp contrast, during retraction of the
320 task irrelevant licks, both the CS and the SS rates were modulated below baseline by amounts that were
321 roughly comparable to the rates of the task relevant licks. That is, the fundamental difference in the P-
322 cell activity between the tube directed and grooming licks was in the protraction phase, but not
323 retraction. This suggests that the difference in the engagement of the P-cells during these two kinds of
324 licks was unlikely to be due to kinematics (i.e., velocity).
325 In summary, the CS-on direction across the P-cells was protraction, whereas CS-off was
326 retraction. As a result, the CS-on direction in the population aligned with the downstream effects of SS
327 suppression, i.e., protrusion. The SS rates peaked during protraction, and were greater when the
328 movement had greater speed or required a greater period of deceleration. In contrast, grooming licks
329 exhibited little or no CS and SS modulation during protraction.
330
331 **Discussion**
332 What does the cerebellum contribute to control of tongue movements? Here, we found that when an
333 olivary input arrived at a P-cell, the resulting suppression prevented the normal deceleration of the
334 tongue as it approached the target, resulting in hypermetria. When the same suppression occurred
335 during retraction, the tongue's return was slowed. These results were consistent for both ipsilateral and
336 contralateral targets. Notably, if the suppression was present in pairs of simultaneously recorded P-cells,
337 the effects were magnified. Thus, regardless of whether the P-cell suppression occurred during
338 protraction or retraction, the downstream effects were forces that pulled the tongue outwards. Because
339 during unperturbed movements the SS rates reached their maximum at peak velocity of protraction, we
340 infer that the consequence of this activity was to decelerate the tongue. This implies that the
341 contributions of the cerebellum to control of tongue movements are similar to that of the eyes (27, 28)
342 and the limbs (29): stopping the movement on target.
343 Like the SS rates, the CS rates peaked near protraction peak velocity, then fell below baseline
344 before the onset of retraction. Thus, for both ipsilateral and contralateral movements, the "CS-on
345 action" across the P-cells was protrusion, while the "CS-off action" was retraction. Notably, the

346 downstream effects of SS suppression were to extend the tongue. Thus, there was a correspondence
347 between the vector that described the CS-on action, and the vector that described the effects of SS
348 suppression. This fact is notable because the same principle holds for P-cells in the oculomotor region of
349 the cerebellum during saccadic eye movements (21): the olivary input to an oculomotor P-cell is most
350 active when a saccade is planned in direction CS-on, and the downstream effects of that P-cell's SS
351 suppression is to pull the eyes also in direction CS-on. Thus, for both eye movements and tongue
352 movements, the olivary input dictates a coordinate system with which to decode the downstream
353 contributions of a P-cell to control of that movement (30, 31).
354 Notably, not all tongue movements engaged the cerebellum. Rather, when the purpose of the
355 movement was to groom the face, during the protraction phase the CS rates remained at baseline while
356 the SS modulations were reduced. Similarly, during task relevant saccades both the CS and the SS rates
357 were strongly modulated, whereas during task irrelevant saccades the CS rates were at baseline and the
358 SS modulations were damped (15, 16). Thus, the strong engagement of the inferior olive and the P-cells
359 during precision tongue movements were missing during grooming licks.
360
361 *The origin of climbing fiber activity at movement onset*
362 We were surprised that the CS rates peaked not after the tongue contacted the tube, but around the
363 time that the protraction began. This observation reproduced findings of Welsh et al. (10) in rats, who
364 recorded from the lateral cerebellum and found that the CS rates peaked near the onset of tongue
365 protrusion, even when the tongue was deafferented. Indeed, in many types of movements, including
366 walking (32), reaching (33–37), and moving the wrist (38), the CS rates peak near movement onset. For
367 example, in the oculomotor vermis, near saccade onset the olivary input informs the P-cells regarding
368 the direction of the upcoming movement (15). How might the inferior olive be involved in transmitting
369 movement information to the cerebellum?
370 A key observation is that the inferior olive not only receives input from the superior colliculus
371 (39–41), but that subthreshold stimulation of a region of the colliculus leads to CS production without
372 producing a movement (42). Thus, it is possible that the increased CS rates around the onset of
373 protraction reflect activities of regions that initiated the tongue movement, i.e., the motor cortex and
374 the superior colliculus (43). This prediction remains to be tested with simultaneous recordings from the
375 colliculus, motor cortex, and the cerebellum.
376
377 *Preparing to initiate a tongue movement coincided with ramping activity in the P-cells*
378 As the subject prepared to initiate a licking bout, the P-cells exhibited a ramping activity. Previous
379 reports have noted that during this period there is ramping activity in the tongue regions of the motor
380 cortex (44), as well as in the fastigial (44) and the dentate nuclei (45). Inhibiting the fastigial during the
381 ramping period disrupts planning of the movement and removes the selectivity that the motor cortical
382 cells exhibit for direction of tongue movements (44), while inhibiting the dentate disrupts the ramping
383 activity in the motor cortex (45). Similarly, exciting the P-cells in the vermis abolishes the ramping
384 activity in motor cortex during the delay period of a decision-making task (46). This implies that as one
385 prepares to initiate a movement, the rising activity in the motor cortex is controlled via a loop through
386 the cerebellum. Because most of the P-cells in the vermis exhibited increasing activity during the delay
387 period, we speculate that their role is to reduce the rate of rise in the motor cortex, effectively delaying
388 the onset of the bout.

Using the olivary input to infer P-cell contributions to control of behavior

Complex spikes are rare neural events, occurring at around once per second. They briefly and completely suppress the SS rates, which induce downstream effects on the cerebellar nuclei (47), potentially producing movements (19). However, the CS rates are modulated to encode the direction of sensory prediction errors (12, 15, 48, 49). Thus, it was critical to test that the kinematic effects that we measured following a CS-induced SS suppression were not a consequence of a feedback response to kinematic deviations that occurred before the CS.

We did this by comparing triplets of temporally adjacent licks, finding that while the kinematics preceding the CS event remained within the chance error bounds, the kinematics that followed were robustly different than chance. Notably, the downstream effects of the CS-induced suppression were in the same direction, i.e., extension of the tongue, regardless of whether the CS events occurred during protraction or retraction. This is notable because the CS rates were maximum during protraction, and minimum during retraction, yet their kinematic effects were the same.

The idea that the olivary input can alter ongoing movements was noted by Ebner and colleagues during reaching movements (20), and subsequently observed during saccades (21). For example, during saccades following the CS-induced SS suppression, the eyes are pulled in the CS-on direction of the P-cell. This is consistent with the fact that optogenetic increase in the SS rates suppresses the cerebellar nuclei (50), pulling the eyes approximately in direction CS+180 (51). While relying on the stochasticity in the olivary input has the disadvantage of lacking a causal manipulation, it has the advantage of relating the kinematic effects to CS-on properties of each P-cell, something that would not be possible with large scale optogenetic stimulation.

Methods

Data were collected from three marmosets, *Callithrix Jacchus*, 2 male and 1 female, 350-370 g, subjects 125D (Mirza), 59D (Ramon), and 132F (Charlie), during a 3.5-year period. The marmosets were born and raised in a colony that Prof. Xiaoqin Wang has maintained at the Johns Hopkins School of Medicine since 1996. The procedures on the marmosets were approved by the Johns Hopkins University Animal Care and Use Committee in compliance with the guidelines of the United States National Institutes of Health.

Data acquisition

Following recovery from head-post implantation surgery, the animals were trained to make saccades to visual targets and rewarded with a mixture of applesauce and lab diet (24). Visual targets were presented on an LCD screen. Binocular eye movements were tracked at 1000 Hz using EyeLink in subject R and M, and 2000 Hz using VPIX in subject C. Tongue movements were tracked with a 522 frame/sec Sony IMX287 FLIR camera, with frames captured at 100 Hz.

We performed MRI and CT imaging on each animal and used the imaging data to design an alignment system that defined trajectories from the burr hole to various locations in the cerebellar vermis (24), including points in lobule VI and VII. We used a piezoelectric, high precision microdrive (0.5 micron resolution) with an integrated absolute encoder (M3-LA-3.4-15 Linear smart stage, New Scale Technologies) to advance the electrode.

We recorded from the cerebellum using quartz insulated 4 fiber (tetrode) or 7 fiber (heptode) metal core (platinum/tungsten 95/05) electrodes (Thomas Recording), and 64 channel checkerboard or linear high density silicon probes (M1 and M2 probes, Cambridge Neurotech). We connected each electrode to a 32 or 64 channel head stage amplifier and digitizer (RHD2132 and RHD2164, Intan Technologies, USA), and then connected the head stage to a communication system (RHD2000 Evaluation Board, Intan Technologies, USA). Data were sampled at 30 kHz and band-pass filtered (2.5 - 7.6 kHz).

Behavioral protocol

Each trial began with fixation of a center target after which a primary target appeared at one of 8 randomly selected directions at a distance of 5-6.5 deg. As the subject made a saccade to this primary target, that target was erased, and a secondary target was presented at a distance of 2-2.5 deg, also at one of 8 randomly selected directions. The subject was rewarded if following the primary saccade, it made a corrective saccade to the secondary target, landed within 1.5 deg radius of the target center, and maintained fixation for at least 200 ms. The food was provided in two small tubes (4.4 mm diameter), one to the left and the other to the right of the animal. A successful trial produced a food increment in one of the tubes and would continue to do so for 50-300 consecutive trials, then switch to the other tube. Because the food increment was small, the subjects naturally chose to work for a few consecutive trials, tracking the visual targets and allowing the food to accumulate, then stopped tracking and harvested the food via a licking bout. The subjects did not work while harvesting, and often fixated the tube. As a result, the behavior consisted of a work period of targeted saccades, followed by a harvest period of targeted licking, repeated hundreds of times per session.

We analyzed tongue movements using DeepLabCut(52). Our network was trained on 89 video recordings of each subject with 15-25 frames extracted and labeled from each recording. The network was built on the ResNet-152 prE-trained model, and then trained over 1.03x106 iterations with a batch size of 8, using a GeForce GTX 1080Ti graphics processing unit. A Kalman filter was further applied to

improve quality and smoothness of the tracking, and the output was analyzed in MATLAB to quantify varying lick events and kinematics. We tracked the tongue tip and the edge of the food in the tube, along with control locations (nose position and tube edges). We tracked all licks, regardless of whether they were aimed toward a tube, or not.

Neurophysiological analysis

We used OpenEphys (53) for electrophysiology data acquisition, and then used P-sort (25) to identify the simple and complex spikes in the heptodes and tetrodes recordings, and Kilosort and Phi (54) to identify the spikes for the silicon probes. Simple and complex spike instantaneous firing rate were calculated from peri-event time histograms with 1 ms bin size. We used a Savitzky–Golay filter (2nd order, 31 datapoints) to smooth the traces for visualization purposes. CS baseline firing rates were computed by dividing the total number of spikes by the duration of the entire recording. SS baseline firing rates were computed using two different methods depending on the analysis. For bout related responses, baseline was defined as the average firing rate in a 300 ms window preceding bout onset by 700 ms, i.e. during the [-1000 to -700] ms. However, to analyze the activities during individual licks, because the rates were not stationary but gradually changing from the first to the last lick in the bout, baseline SS rates were computed using the average firing within a sliding window of 2 seconds, consisting of roughly 5 licks.

Computing the kinematic effects of CS-induced SS suppression

For each P-cell we considered triplets of consecutive tubE-directed licks $\{n-1, n, n+1\}$, where all three licks were of the same type, i.e., contacted the same part of the tube (edge or inner). We then selected the subset of triplets in which there was a CS at only a single period in lick n, but no CS during all periods in the two neighboring licks $n-1$, and $n+1$. We then compared tongue trajectories between the lick that had a CS with the two neighboring licks, i.e., $n-(n-1)$ and $n-(n+1)$.

Statistical analysis

In order to compute the bounds for the null hypothesis, we used bootstrapping to compute 95% confidence intervals. We shuffled the assignment of CS tags from the lick in which it had occurred to a randomly assigned lick of the same type. Using this pseudo-data, we then selected triplets of consecutive tubE-directed licks and computed trajectory differences among neighboring licks, averaging $n-(n-1)$ and $n-(n+1)$. We computed this expected value for each cell, computed a mean across all the cells, and then repeated the shuffling 30 times to compute 95% confidence intervals.

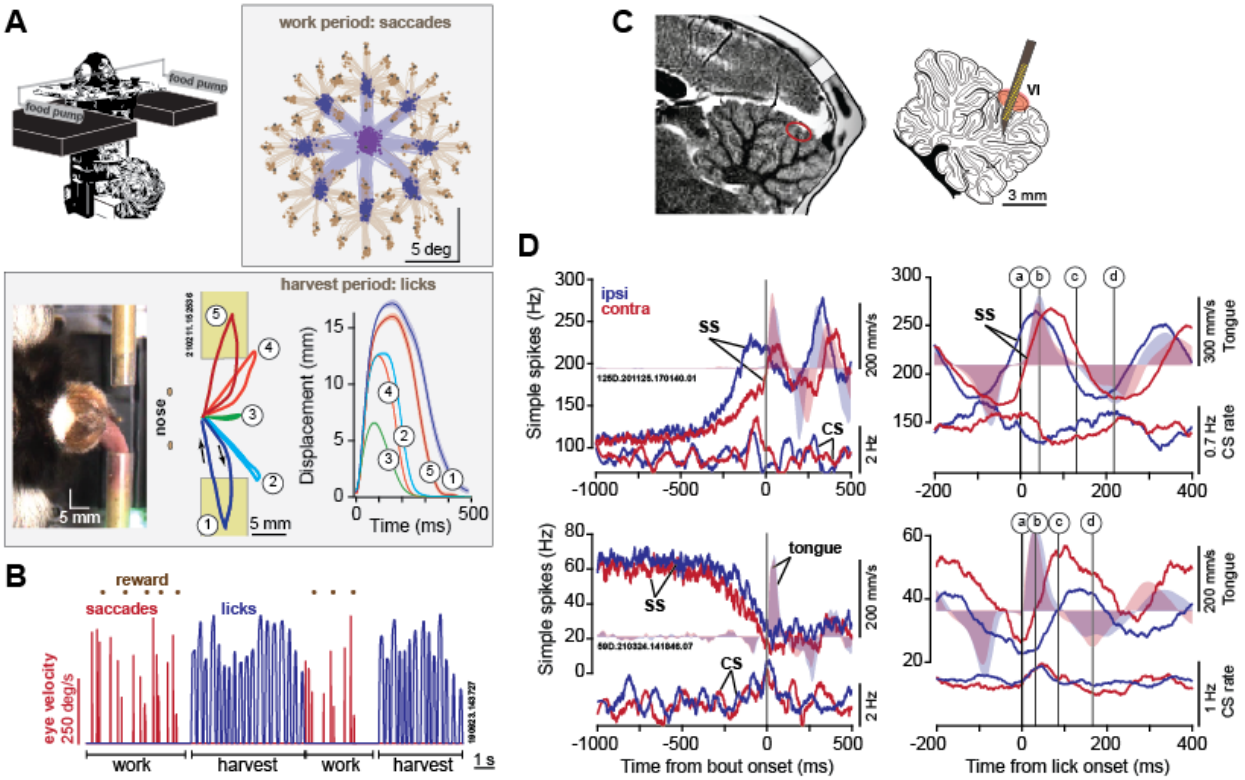

Figure 1. Marmosets produced dexterous tongue movements during recordings from lobule VI of the cerebellar vermis. A. Subjects made saccades to visual targets and received a small amount of food as reward via one of two tubes placed obliquely to the mouth. In the task relevant licks, they directed their tongue to the edge of the tube to harvest food near the tip (trajectories 2, 4), or inside the tube to harvest food that was deeper (trajectories 1, 5). In task irrelevant licks, they groomed their face (trajectory 3). **B**. Subjects chose to work for consecutive trials, making saccades and allowing the food to accumulate, then harvested the food in bouts of licking. **C**. We employed silicon probes to record from lobule VI of the vermis. **D**. Simple and complex spikes (SS, CS) of two Purkinje cells, aligned to bout onset and lick onset. A single lick was divided into acceleration period of protraction (a-b), deceleration period of protraction (b-c), and acceleration period of retraction (c-d). Filled color regions indicate tongue velocity.

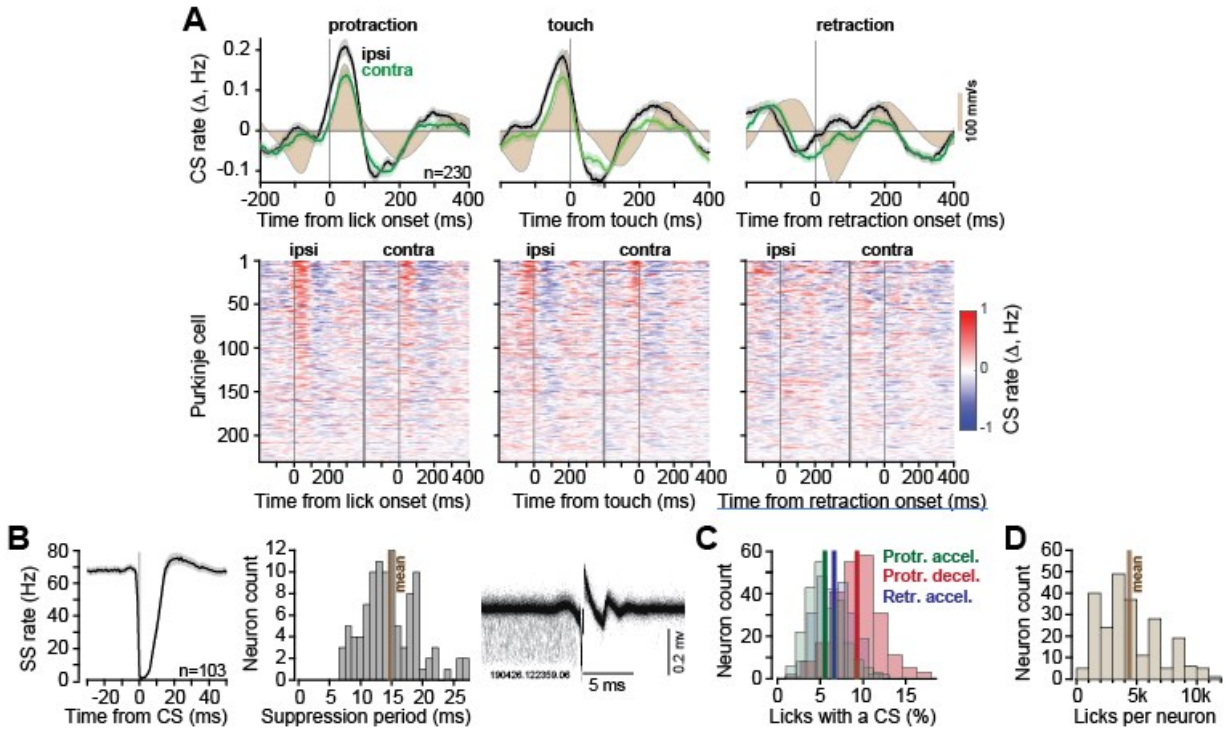

Figure 2. CS rates increased with protraction and decreased with retraction. A. CS rates across the population aligned to protraction onset, touch of the tube, and retraction onset. **B**. CS-induced SS suppression, averaged across the subset of P-cells for which both the CS and the SS were isolated (left). Examples of SS and CS waveforms for a single P-cell are shown at right. **C**. CS activity across all P-cells, aligned to protraction, touch, and retraction, sorted based on CS rate for contralateral licks at lick onset. **D**. Percentage of licks with a CS during a specific period of time for each neuron. **E**. Number of task relevant licks per neuron. Error bars are SEM.

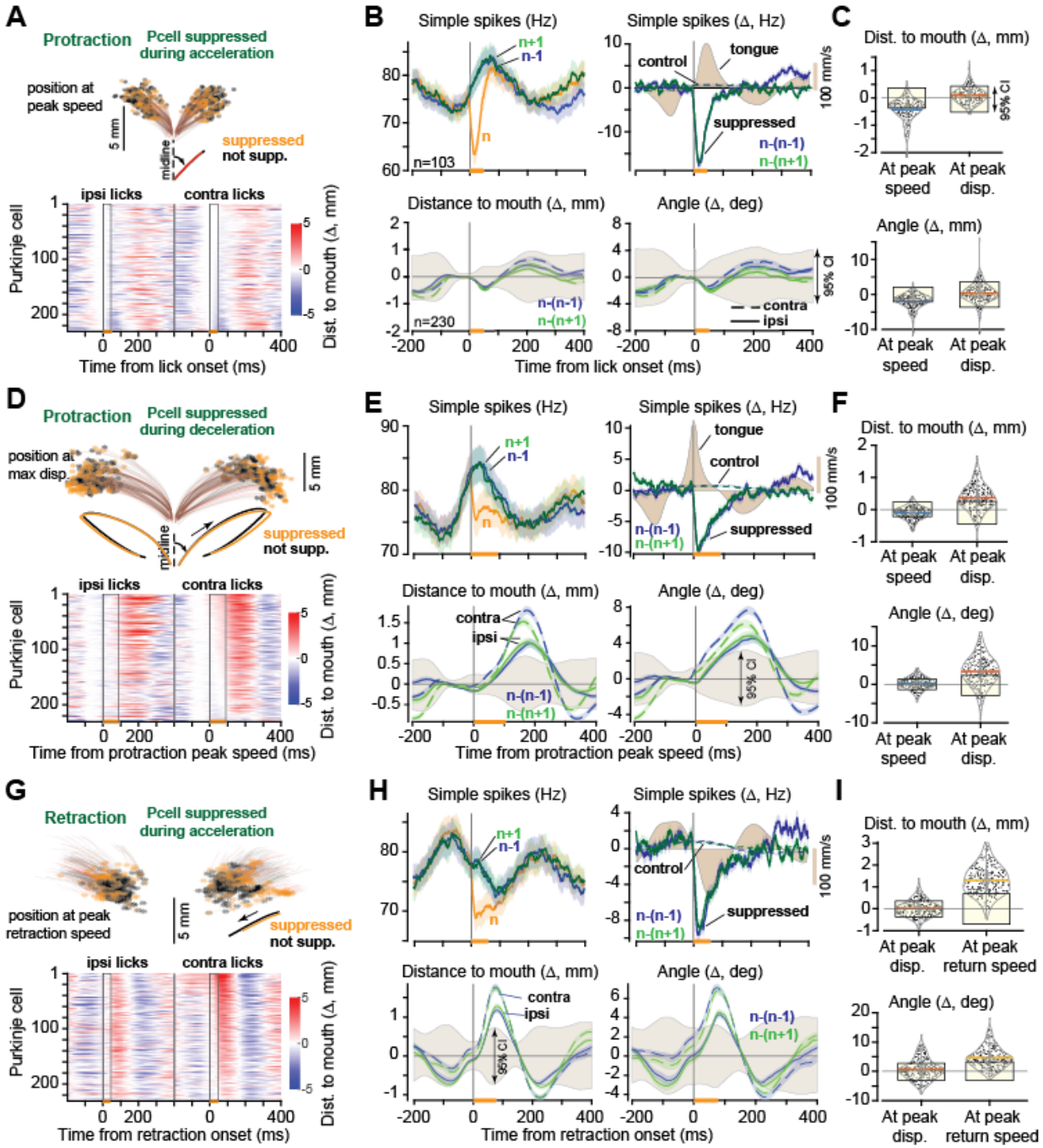

Figure 3. CS-induced SS suppression produced hypermetria during protraction and slowing during retraction. A. Suppression during the acceleration period of protraction (orange bar). Traces show average tongue trajectory for each P-cell during suppressed and control licks. Ipsilateral licks are shown to the left and contralateral to the right. Heatmap quantifies change in endpoint trajectory between suppressed and control licks for each cell. **B**. Top row: SS rates for licks $\{n-1, n, n+1\}$, where only lick n experienced a CS. Filled color curves indicate tongue velocity. Second row: trajectory of the tongue in lick n as compared to its two temporally neighboring licks. Trajectory is measured via distance from tip of the tongue to the mouth and angle of the tip with respect to midline. The filled region is 95% CI. **C**. Distance to mouth and angle in lick n as compared to neighboring licks. Shaded region is 95% CI. **D-F**. Suppression during the deceleration period of protraction induces hypermetria. Same format as in part A-

C. **G-I.** Suppression during the acceleration period of retraction induces slowing. Same format as in part A-C. Error bars are SEM.

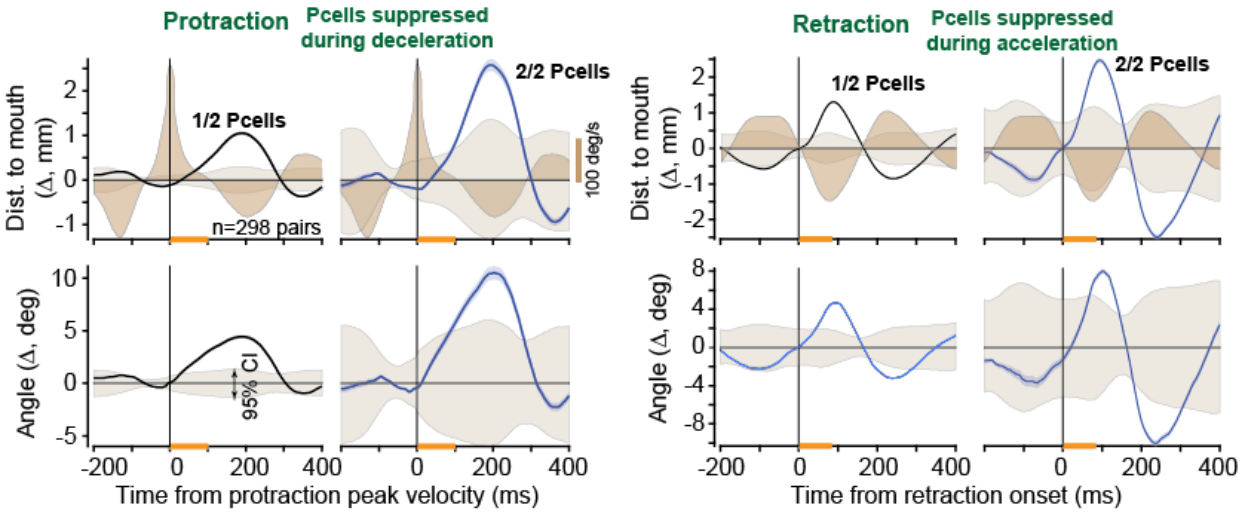

Figure 4. Suppression of multiple P-cells scaled the perturbation to the tongue. **A**. Kinematic effects of CS-induced P-cell suppression during the deceleration period of protraction (orange bar). Traces show change in tongue trajectory in suppressed licks vs. control licks, measured via distance from tip of the tongue to the mouth and angle of the tip with respect to midline. Gray shaded region is 95% CI. Brown filled region is tongue velocity. **B**. Kinematic effects of P-cell suppression during the acceleration period of retraction (orange bar). Same format as in part A. Error bars are SEM.

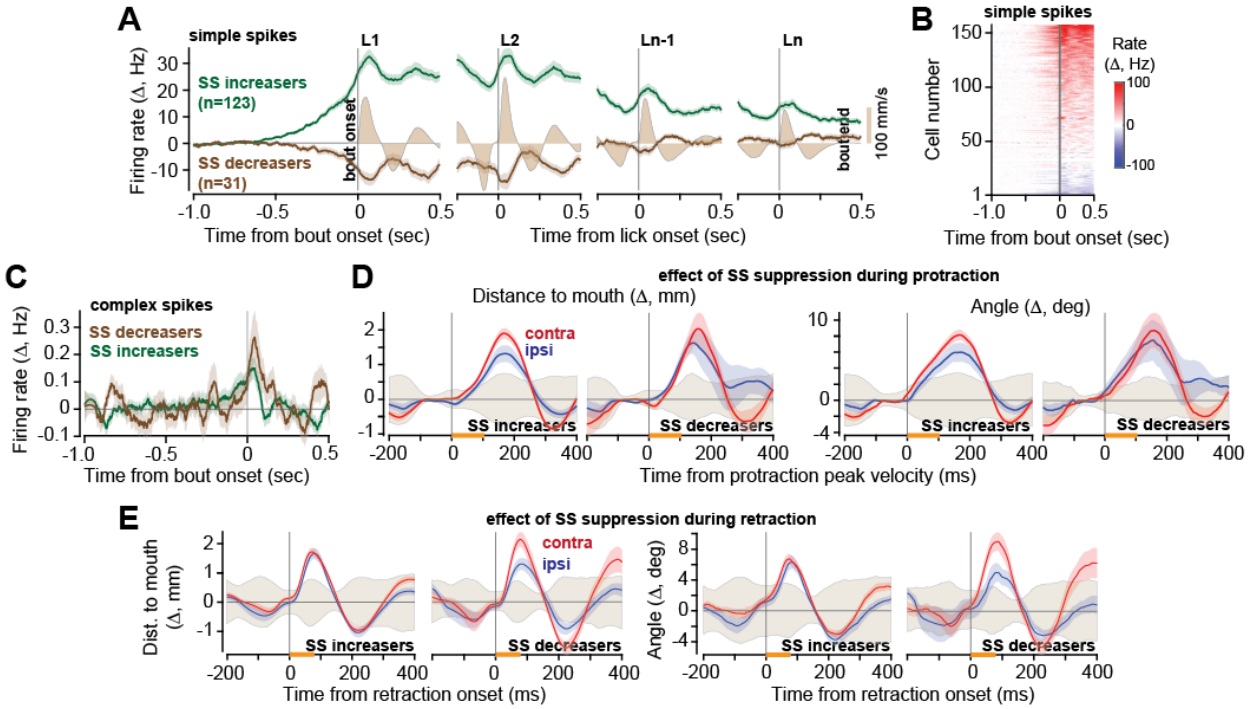

Figure 5. Effects of suppression remained consistent across P-cells regardless of SS modulation. A. Some of the P-cells exhibited an increase in SS rates before bout onset, while others exhibited a decrease. L1 is first lick in the bout, Ln is last lick. **B**. Change in SS rates for all P-cells (with respect to baseline), aligned to bout onset. **C**. Change in complex spike rate for the same P-cells. **D**. Kinematic effects of SS suppression during the deceleration period of protraction (orange bar). Shaded region is 95% CI. E. Kinematic effects of SS suppression during the acceleration period of retraction (orange bar). Error bars are SEM.

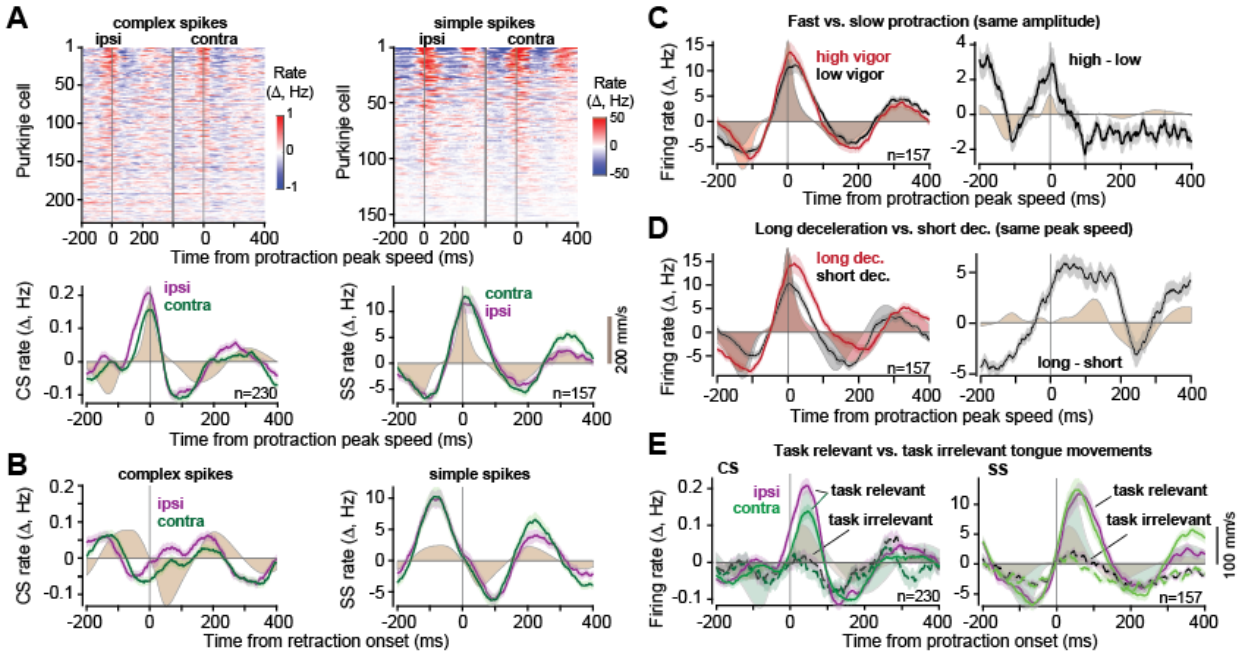

Figure 6. SS rates were greater for high vigor and long deceleration licks. **However, little modulation was present during task irrelevant tongue movements. A**. CS and SS rates across the population aligned to protraction peek speed. As a population, the direction of CS-on was protraction. **B**. CS and SS rates aligned to retraction onset. **C**. Left figure shows SS rates for high and low vigor protractions (same amplitude). Right figure shows within cell difference in SS rates for high minus low vigor licks. Shaded regions are tongue speed for high and low vigor licks (left) and change in speed (right). **D**. Left figure shows SS rates for protractions that long or short deceleration periods but the same peak speed. Right figure shows within cell differences. Shaded regions are tongue speed for long and short deceleration period licks (left) and change in speed (right). **E**. Modulation of CS and SS rates during task relevant and task irrelevant licks. Light shaded region is tongue speed for task relevant movements, while dark shaded region is tongue speed for task irrelevant movements. Error bars are SEM.

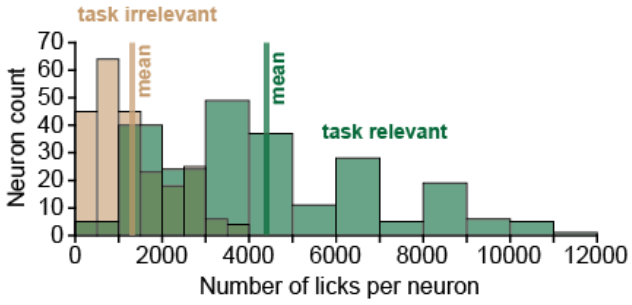

Supplementary Figure 1. The number of task relevant (tube directed) and task irrelevant (grooming) licks recorded per neuron.

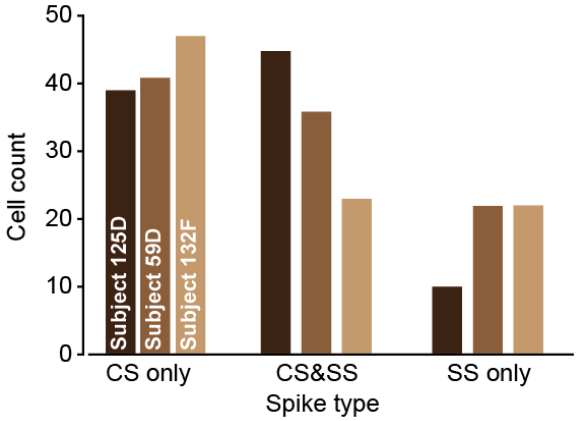

Supplementary Figure 2. The number of neurons recorded from each marmoset. CS only refers to P-cells for which only the complex spikes were recorded. CS&SS refers to P-cells for which both the CS and SS were recorded. SS only refers to putative P-cells for which only the SS were recorded.

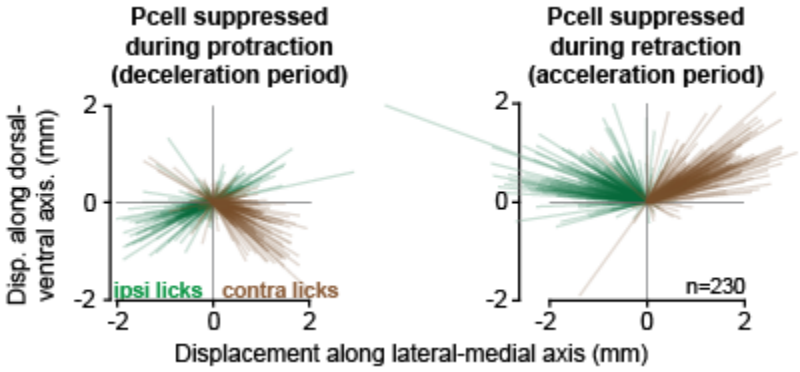

Supplementary Figure 3. Kinematic effects of CS-induced P-cell suppression in Cartesian coordinates. Left plot shows the change in the position of the tip of the tongue at the end of protraction in movements that experienced a CS during the deceleration period of protraction, with respect to movements that did not experience a CS during any period. Right plot shows the change in position of the tip of the tongue as measured at peak retraction velocity, comparing movements that experienced a CS during the retraction acceleration period with movements that did not experience a CS in any period. Each line is the average effect for a single P-cell. P-cell suppression during protraction produced hypermetria, whereas the suppression during retraction resulted in slowing.

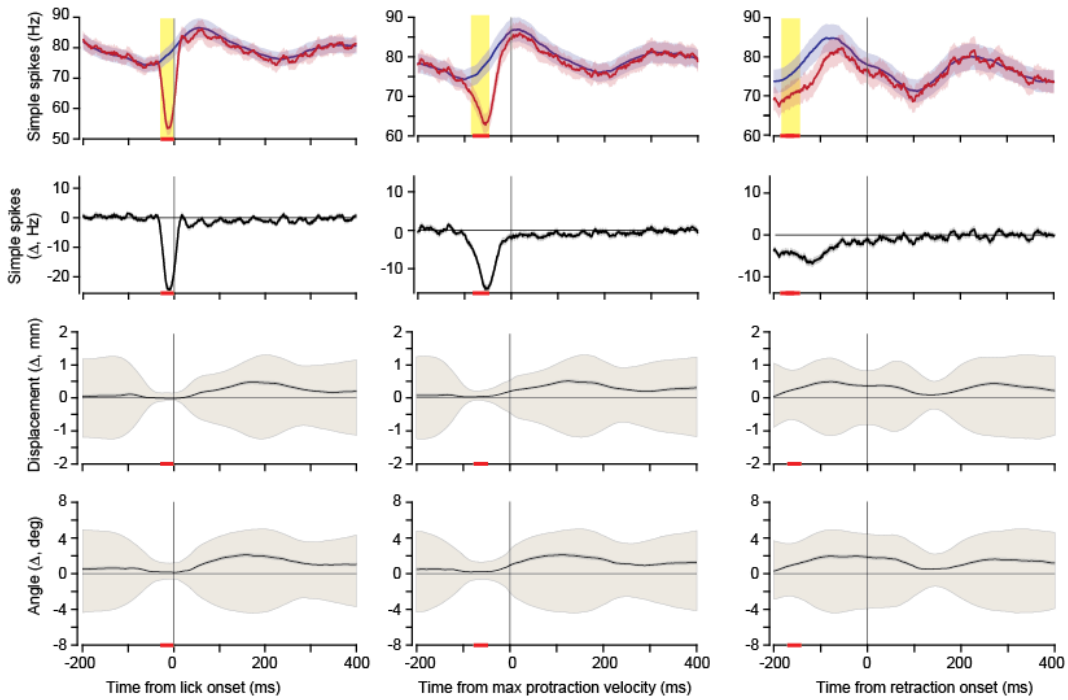

Supplementary Figure 4. There was little or no change in lick kinematics when the CS-induced SS suppression occurred before lick onset. We chose the period following completion of one lick and the start of the next lick, which was on average 30ms in duration, i.e., the period in which the tongue was in the mouth. Top row: SS rates, aligned to lick onset, protraction peak speed, and retraction onset. Second row: change in SS rates. Third row: change in tongue displacement. Fourth row: change in tongue angle. The filled region is 95% confidence interval. Error bars are SEM.

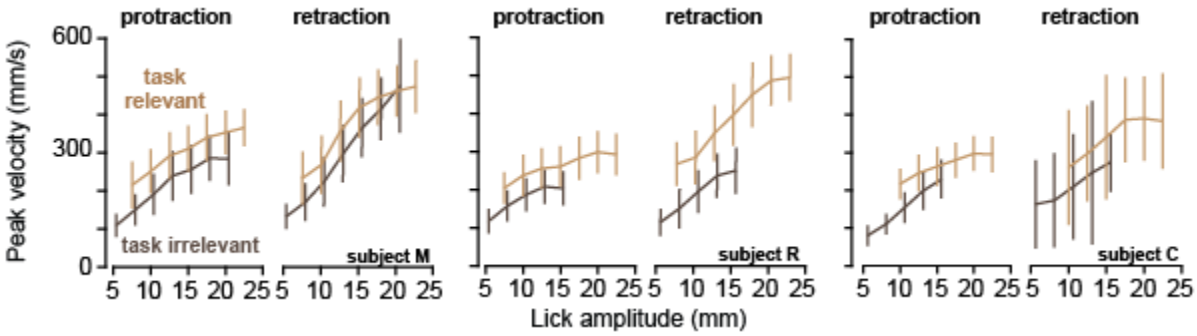

Supplementary Figure 5. Peak velocity as a function of lick amplitude during protraction and retraction for task relevant and task irrelevant licks in each subject. Error bars are SEM.

583 1. W. J. M. Levelt, *Speaking: From Intention to Articulation* (MIT Press, 1993).

584 2. M. Gentil, EMG analysis of speech production of patients with Friedreich disease. *Clin. Linguist.*
585 *Phon.* **4**, 107–120 (1990).

586 3. T. Vilis, J. Hore, Central neural mechanisms contributing to cerebellar tremor produced by limb
587 perturbations. *J.Neurophysiol.* **43**, 279–291 (1980).

588 4. F. Yu, Q. J. Jiang, X. Y. Sun, R. W. Zhang, A new case of complete primary cerebellar agenesis:
589 clinical and imaging findings in a living patient. *Brain* **138**, e353 (2015).

590 5. J. L. Bryant, J. D. Boughter, S. Gong, M. S. LeDoux, D. H. Heck, Cerebellar cortical output encodes
591 temporal aspects of rhythmic licking movements and is necessary for normal licking frequency.
592 *Eur. J. Neurosci.* **32**, 41–52 (2010).

593 6. M. A. Gaffield, J. M. Christie, Movement Rate Is Encoded and Influenced by Widespread, Coherent
594 Activity of Cerebellar Molecular Layer Interneurons. *J.Neurosci.* **37**, 4751–4765 (2017).

595 7. J. P. Bowman, L. D. Aldes, Organization of the cerebellar tongue representation in the monkey.
596 *Exp. Brain Res.* **39**, 249–259 (1980).

597 8. L. D. Aldes, J. P. Bowman, Representation of the tongue in the cerebellar nuclei of the monkey.
598 *Exp. Neurol.* **64**, 202–215 (1979).

599 9. M. A. Gaffield, B. A. Sauerbrei, J. M. Christie, Cerebellum encodes and influences the initiation,
600 performance, and termination of discontinuous movements in mice. *eLife* **11**, e71464 (2022).

601 10. J. P. Welsh, E. J. Lang, I. Suglhara, R. Llinas, Dynamic organization of motor control within the
602 olivocerebellar system. *Nature* **374**, 453–457 (1995).

603 11. K. Kubota, S. Hayama, Comparative anatomical and neurohistological observations on the tongues
604 of pigmy and common marmosets. *Anat. Rec.* **150**, 473–485 (1964).

605 12. D. J. Herzfeld, Y. Kojima, R. Soetedjo, R. Shadmehr, Encoding of error and learning to correct that
606 error by the Purkinje cells of the cerebellum. *Nat.Neurosci.* **21**, 736–743 (2018).

607 13. C. Ju, *et al.*, Neurons of the inferior olive respond to broad classes of sensory input while subject to
608 homeostatic control. *J. Physiol.* **597**, 2483–2514 (2019).

609 14. S. Tsutsumi, *et al.*, Purkinje Cell Activity Determines the Timing of Sensory-Evoked Motor Initiation.
610 *Cell Rep.* **33**, 108537 (2020).

611 15. J. S. Pi, *et al.*, The olivary input to the cerebellum dissociates sensory events from movement plans.
612 *Proc. Natl. Acad. Sci.* **121**, e2318849121 (2024).

613 16. E. Sedaghat-Nejad, J. S. Pi, P. Hage, M. A. Fakharian, R. Shadmehr, Synchronous spiking of
614 cerebellar Purkinje cells during control of movements. *Proc. Natl. Acad. Sci.* **119**, e2118954119
615 (2022).

616 17. Y. Sato, A. Miura, H. Fushiki, T. Kawasaki, Short-term modulation of cerebellar Purkinje cell activity
617 after spontaneous climbing fiber input. *J. Neurophysiol.* **68**, 2051–2062 (1992).

618 18. W. T. Thach, Somatosensory receptive fields of single units in cat cerebellar cortex. *J.Neurophysiol.*
619 **30**, 675–696 (1967).

620 19. V. Romano, *et al.*, Olivocerebellar control of movement symmetry. *Curr. Biol.* **32**, 654-670.e4
621 (2022).

622 20. M. L. Streng, L. S. Popa, T. J. Ebner, Climbing Fibers Control Purkinje Cell Representations of
623 Behavior. *J.Neurosci.* **37**, 1997–2009 (2017).

624 21. S. Z. Muller, *et al.*, Complex spikes perturb movements and reveal the sensorimotor map of
625 Purkinje cells. *Curr. Biol.* **33**, 4869-4879.e3 (2023).

626 22. P. Hage, *et al.*, Effort cost of harvest affects decisions and movement vigor of marmosets during
627 foraging. *eLife* **12**, RP87238 (2023).

628 23. A. Mathis, *et al.*, DeepLabCut: markerless pose estimation of user-defined body parts with deep
629 learning. *Nat. Neurosci.* **21**, 1281–1289 (2018).

630 24. E. Sedaghat-Nejad, *et al.*, Behavioral training of marmosets and electrophysiological recording
631 from the cerebellum. *J.Neurophysiol.* **122**, 1502–1517 (2019).

632 25. E. Sedaghat-Nejad, *et al.*, P-sort: an open-source software for cerebellar neurophysiology. *J.*
633 *Neurophysiol.* **126**, 1055–1075 (2021).

634 26. T. R. Reppert, *et al.*, Movement vigor as a trait-like attribute of individuality. *J.Neurophysiol.* **120**,
635 741–757 (2018).

636 27. Y. Kojima, F. R. Robinson, R. Soetedjo, Cerebellar fastigial nucleus influence on ipsilateral abducens
637 activity during saccades. *J.Neurophysiol.* **111**, 1553–1563 (2014).

638 28. C. Bourrelly, J. Quinet, L. Goffart, The caudal fastigial nucleus and the steering of saccades toward
639 a moving visual target. *J. Neurophysiol.* **120**, 421–438 (2018).

640 29. M. I. Becker, A. L. Person, Cerebellar Control of Reach Kinematics for Endpoint Precision. *Neuron*
641 **103**, 335–348 (2019).

642 30. T. J. H. Ruigrok, J. Voogd, Organization of projections from the inferior olive to the cerebellar nuclei
643 in the rat. *J. Comp. Neurol.* **426**, 209–228 (2000).

644 31. R. Apps, M. Garwicz, Anatomical and physiological foundations of cerebellar information
645 processing. *Nat.Rev.Neurosci.* **6**, 297–311 (2005).

646 32. T. M. Hoogland, J. R. De Gruijl, L. Witter, C. B. Canto, C. I. De Zeeuw, Role of Synchronous
647 Activation of Cerebellar Purkinje Cell Ensembles in Multi-joint Movement Control. *Curr. Biol.* **25**,
648 1157–1165 (2015).

649 33. S. Kitazawa, T. Kimura, P. B. Yin, Cerebellar complex spikes encode both destinations and errors in
650 arm movements. *Nature* **392**, 494 (1998).

651 34. A. L. Hewitt, L. S. Popa, T. J. Ebner, Changes in Purkinje cell simple spike encoding of reach
652 kinematics during adaption to a mechanical perturbation. *J.Neurosci.* **35**, 1106–1124 (2015).

653 35. W. Heffley, *et al.*, Coordinated cerebellar climbing fiber activity signals learned sensorimotor
654 predictions. *Nat. Neurosci.* **21**, 1431–1441 (2018).

655 36. M. J. Wagner, *et al.*, A neural circuit state change underlying skilled movements. *Cell* **184**, 3731-
656 3747.e21 (2021).

657 37. D. J. Calame, M. I. Becker, A. L. Person, Cerebellar associative learning underlies skilled reach
658 adaptation. *Nat. Neurosci.* 1–12 (2023). https://doi.org/10.1038/s41593-023-01347-y.

659 38. T. Ishikawa, *et al.*, Releasing dentate nucleus cells from Purkinje cell inhibition generates output
660 from the cerebrocerebellum. *PLoS.One.* **9**, e108774 (2014).

661 39. Y. Kojima, R. Soetedjo, Change in sensitivity to visual error in superior colliculus during saccade
662 adaptation. *Sci.Rep.* **7**, 9566 (2017).

663 40. Y. Kojima, R. Soetedjo, Elimination of the error signal in the superior colliculus impairs saccade
664 motor learning. *Proc.Natl.Acad.Sci.U.S.A* **115**, E8987–E8995 (2018).

665 41. P. J. May, S. Warren, Y. Kojima, The superior colliculus projection upon the macaque inferior olive.
666 *Brain Struct. Funct.* (2024). https://doi.org/10.1007/s00429-023-02743-7.

667 42. R. Soetedjo, Y. Kojima, A. F. Fuchs, How cerebellar motor learning keeps saccades accurate. *J.*
668 *Neurophysiol.* **121**, 2153–2162 (2019).

669 43. A. Thomas, *et al.*, Superior colliculus bidirectionally modulates choice activity in frontal cortex. *Nat.*
670 *Commun.* **14**, 7358 (2023).

671 44. Z. Gao, *et al.*, A cortico-cerebellar loop for motor planning. *Nature* **563**, 113–116 (2018).

672 45. F. P. Chabrol, A. Blot, T. D. Mrsic-Flogel, Cerebellar Contribution to Preparatory Activity in Motor
673 Neocortex. *Neuron* **103**, 506–519 (2019).

674 46. J. Zhu, H. Hasanbegović, L. D. Liu, Z. Gao, N. Li, Activity map of a cortico-cerebellar loop underlying
675 motor planning. *Nat. Neurosci.* 1–13 (2023). https://doi.org/10.1038/s41593-023-01453-x.

676 47. T. Tang, T. A. Blenkinsop, E. J. Lang, Complex spike synchrony dependent modulation of rat deep
677 cerebellar nuclear activity. *eLife* **8**, e40101 (2019).

678 48. J. F. Medina, S. G. Lisberger, Links from complex spikes to local plasticity and motor learning in the
679 cerebellum of awake-behaving monkeys. *Nat.Neurosci.* **11**, 1185–1192 (2008).

680 49. Y. Yang, S. G. Lisberger, Role of Plasticity at Different Sites across the Time Course of Cerebellar
681 Motor Learning. *J. Neurosci.* **34**, 7077–7090 (2014).

682 50. J. Chaumont, *et al.*, Clusters of cerebellar Purkinje cells control their afferent climbing fiber
683 discharge. *Proc.Natl.Acad.Sci.U.S.A.* **110**, 16223–16228 (2013).

684 51. R. Soetedjo, G. D. Horwitz, Closed-Loop Optogenetic Perturbation of Macaque Oculomotor
685 Cerebellum: Evidence for an Internal Saccade Model. *J. Neurosci.* **44** (2024).

686 52. A. Mathis, *et al.*, DeepLabCut: markerless pose estimation of user-defined body parts with deep
687 learning. *Nat. Neurosci.* **21**, 1281–1289 (2018).

688 53. J. H. Siegle, *et al.*, Open Ephys: an open-source, plugin-based platform for multichannel
689 electrophysiology. *JNeural Eng* **14**, 045003 (2017).

690 54. M. Pachitariu, N. Steinmetz, S. Kadir, M. Carandini, H. K. D, Kilosort: realtime spike-sorting for
691 extracellular electrophysiology with hundreds of channels. *bioRxiv* 061481 (2016).
692 https://doi.org/10.1101/061481.

693
694